
PERGAMON

Journal of Quantitative Spectroscopy & Radiative Transfer 79–80 (2003) 521–531

Journal of Quantitative Spectroscopy & Radiative Transfer

www.elsevier.com/locate/jqsrt

Scattering efficiency of clusters composed by aggregated spheres

Jean-Claude Auger[a,*], Ruben G. Barrera[b,1], Brian Stout[c]

[a] *Centro de Investigación en Polímeros, Grupo COMEX, Blvd Manuel Avila Camacho No. 138, Lomas de Chapultepec, 11560 Mexico DF, Mexico*

[b] *Instituto de Física, UNAM, Apartado Postal 20-364, 01000 Mexico DF, Mexico*

[c] *Institut Fresnel UMR 6133, Faculté des Sciences et Techniques, Centre de Saint Jerôme, 20, 13397 Marseilles Cedex, France*

Received 31 May 2002; accepted 16 August 2002

Abstract

We present a detailed study of the variation of the average scattering cross section of various aggregates of titanium dioxide crystallites as a function of their sizes and shapes. To perform the analysis, we use a recursive T-matrix algorithm that we developed. We show how the aggregation phenomenon can tremendously decrease the local scattering properties of a white paint film and consequently affects its hiding power. We also compare the results with the equivalent spherical volume approximation which is used in particle size analysis using static or dynamic light-scattering methods. We show how the equivalent volume approximation used in those methods should be handled with care.

Keywords: Multiple-scattering; Aggregate; T-matrix

1. Introduction

Coatings are very complex systems that must posses a large number of desirable properties, like an adequate rheology or flow, good adhesion to the substrate and resistance to mechanical abrasion. In the particular case of architectural paints, the visual aspects like opacity, gloss and tinting strength become determinant features. The present work focuses on the opacity of architectural white paint films. Opacity, also called hiding power, is the property that a paint has to hide a surface, and

* Corresponding author. Centro de Investigación en Polímeros, Grupo COMEX, Blvd Manuel Avila Camacho No 138, Lomas de Chapultepec, 11560 México DF, México.

E-mail address: jcauger@cip.org (J.C. Auger).

[1] Consultant at Centro de Investigación en Polímeros, Grupo COMEX.

0022-4073/03/$ - see front matter
doi:10.1016/S0022-4073(02)00305-9

one refers to complete opacity when the light reflected by the film does not contain any optical information about the substrate. At a microscopic scale opacity is due to the multiple-scattering interactions of light with the small pigment particles which are embedded in a transparent matrix. For any given thickness, the stronger the interactions, the better the hiding power.

One way to increase the magnitude of the scattering efficiency is to increase the contrast in index of refraction between the matrix and the pigments. For this reason, titanium dioxide, with an index of refraction of about 2.8 in the visible range, is the most used pigment in white paint formulation. Also, from Mie theory [1], it is known that the magnitude of the scattering efficiency attains its maximum when the size of the pigment is comparable to the wavelength of the incident radiation. Consequently, the optimum size for the titanium dioxide particles is around 0.250 μm, and the scattering efficiency decreases rapidly as the size increases further. Nevertheless, a monodisperse size distribution of pigments cannot be achieved at an industrial scale, and manufacturers therefore supply the paint industry with a narrow size distribution of TiO_2 pigments centered around its optimum value.

From an optical point of view, a white coating can be seen as an inhomogeneous system composed of a high concentration of titanium dioxide crystallites embedded in a polymer resin. A high concentration is necessary in order to attain a suitable hiding power for a reasonable thickness of the paint film. But in a highly concentrated film, the individual scattering phenomena are no longer independent of each other, a regime known as dependent scattering. It is also known that in the dependent-scattering regime the scattering efficiency of the pigment generally decreases. Moreover, due to Van der Waals attractive forces, the titanium dioxide crystallites tend to form aggregates during storage, production and drying processes. The presence of these aggregates can be regarded as an extreme case of dependent scattering in localized regions, decreasing the hiding power of the coating.

In order to minimize aggregation (clustering), paint formulators use specific substances, called surfactants, that react with the pigment surface and avoid aggregation through steric (spatial rearrangement of atoms) and electrostatic repulsion. Nevertheless, in practice, clustering cannot be totally eliminated. In this work, we present a study of the scattering properties of TiO_2 clusters as a function of their size and shape. We compare the results with the scattering efficiency of an isolated pigment in order to get a quantitative measure of the clustering effect on paint opacity. We also compare the results with the equivalent-spherical-volume approximation that is used in static or dynamic light-scattering techniques for particle-size analysis.

The scattering properties of the titanium-dioxide aggregates are evaluated through a recursive centered T-matrix algorithm (RCTMA) that has been developed in our group. For simplicity, we will model the rutile titanium dioxide crystallites by spheres. However, in reality this assumption can only be seen as a first approximation. The paper is organized as follows: In Section 2, we perform a simple study that illustrates the influence of particle size on paint opacity. In Section 3, we describe briefly the T-matrix formalism that was used in the calculations. In Section 4, we present and discuss our results, and Section 5 is devoted to conclusions.

2. Preliminary study

A simple evaluation of the total scattering efficiency and the diffuse reflection coefficient can illustrate the influence of the size of the TiO_2 crystallites in the opacity of a white paint. As a

first approximation to the aggregation problem, we will regard the shape of both crystallites and aggregates as spheres following closely a log-normal distribution characterized by an average value r_m and a standard deviation σ. The effects of aggregation can then be regarded as a shift of the average value r_m to larger values. With this model in mind one can calculate, from simple Mie theory, the scattering cross section $C_{\mathrm{sca}}(a)$ of the spheres as a function of their radii a.

Coupled with a simple Kubelka–Munk [2] multiple-scattering approach, the scattering efficiency S (or S parameter) is given, within the photon-diffusion regime and the independent-scattering approximation, as

$$S(a) = \frac{3}{4} f \frac{C_{\mathrm{sca}}(a)}{v_{\mathrm{p}}(a)} [1 - g(a)], \tag{1}$$

where $v_{\mathrm{p}}(a) = 4\pi a^3/3$ is the volume of the particle, f the filling fraction of the pigments and

$$g(a) = \frac{1}{C_{\mathrm{sca}}(a)} \int \frac{\mathrm{d}C_{\mathrm{sca}}(a)}{\mathrm{d}\Omega} \cos\theta \, \mathrm{d}\Omega \tag{2}$$

is the asymmetry parameter that accounts for the anisotropy in the angular distribution of the scattered radiation within the film. Here $\mathrm{d}C_{\mathrm{sca}}(a)/\mathrm{d}\Omega$ is the differential scattering cross section, θ is the azimuth angle measured from the direction of the incident beam, the integration is performed over all solid angles Ω, and by photon-diffusion regime, one simply means that the thickness of the film is much larger than the photon mean free path.

The parameter S measures the fraction of a flux originally traveling within the forward hemisphere which is scattered into the backward hemisphere, and it is proportional to the scattering cross section per unit volume. The values of $g(a)$ lie between $-1 \leqslant g(a) \leqslant 1$, where the values 1 and -1 correspond to full forward- and back-scattering processes, respectively. One now weights the scattering efficiency $S(a)$ by the particle-size distribution $N_{\mathrm{p}}(a)$ in order to get a weighted average of the scattering efficiency as

$$\langle S \rangle = \frac{3}{4} f \frac{\int_0^\infty C_{\mathrm{sca}}(a)[1 - g(a)]N_{\mathrm{p}}(a)\,\mathrm{d}a}{\int_0^\infty v_{\mathrm{p}}(a)N_{\mathrm{p}}(a)\,\mathrm{d}a}, \tag{3}$$

where f is the total filling fraction of spheres while $N_{\mathrm{p}}(a)$ is the normalized size distribution, with $\int_0^\infty N_{\mathrm{p}}(a)\,\mathrm{d}a = 1$.

With this value of $\langle S \rangle$, one is able to evaluate the total diffuse reflectance by solving the KM differential equations with specific boundary conditions at both planar faces of the film. Here we assume diffuse illumination, an external and internal reflectance of fully isotropic diffuse radiation at the illuminated face of the film, and a reflection coefficient of 0.8 for a quasi-white substrate (for all wavelengths under consideration). The index of refraction n_{M} of the resin matrix is taken as $n_{\mathrm{M}} = 1.5$, while the index of refraction of titanium dioxide $n_{\mathrm{p}}(\lambda)$ as a function of wavelength λ is taken from the literature [3].

In Fig. 1a, we display the average scattering efficiency $\langle S \rangle$ as a function of λ for two different particle size distributions, while in Fig. 1b we show the corresponding diffuse reflectance. We assume that the distributions are lognormal with the following parameters: (a) $r_{\mathrm{m},1} = 0.19$ and $\sigma_1 = 1.45$ and (b) $r_{\mathrm{m},2} = 0.22$ and $\sigma_2 = 1.22$. Here $r_{\mathrm{m},i}$ is the mean radius while σ_i is the width. For both distributions the total filling fraction f is 0.2 and the thickness of the film is taken equal to 50 μm. One has to

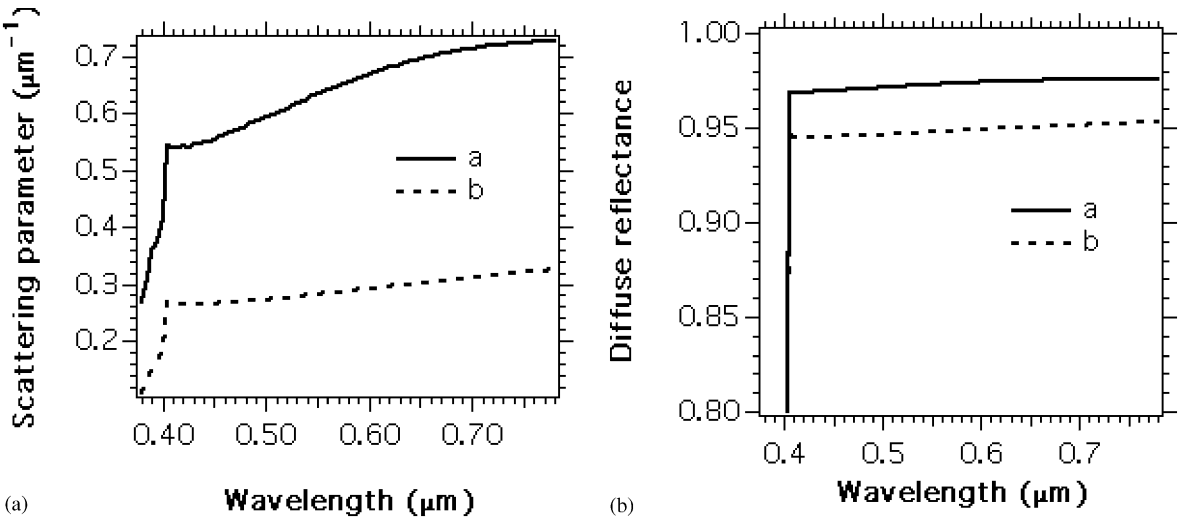

Fig. 1. (a) Scattering efficiency of two size distributions of rutile titanium dioxide pigment: a—size distribution r_m=0.19 μm and $\sigma = 1.45$ and b—size distribution $r_m = 0.22$ μm, $\sigma = 1.22$. (b) Diffuse reflectance of a white paint film. The thickness of the film is 50 μm and the volume fraction of titanium dioxide is 0.2: a—log-normal size distribution with $r_m = 0.19$ μm and $\sigma = 1.45$; and b—log-normal size distribution with $r_m = 0.22$ μm and $\sigma = 1.22$.

notice that $(r_{m,1}, \sigma_1)$ and $(r_{m,2}, \sigma_2)$ are not independent parameters because the total volume occupied by the inclusions has to be identical for both size distributions if one wants describe an aggregation phenomena.

From Figs. 1a and b, one can appreciate how an increase in the mean of the particle-size distribution decreases the scattering efficiency of the pigments, and as a consequence, there is a decreases in the diffuse reflectance, and therefore, in the hiding power. In this calculation, one assumes that all particles are spherical, and the clusters or aggregates are therefore also regarded as homogeneous spheres of a large radius within the non-absorbing matrix. But a question now arises, how the diffuse reflectance changes if instead of regarding the clusters as large spheres one actually calculates the scattering efficiency of the cluster regarded as a specific arrangement of crystallites. As a first approximation we will regard the shape of the crystallites as spherical. It has also been proved that the calculation of the scattering efficiency of clusters of spherical particles can be safely performed using the T-matrix formalism (see for example [4]).

3. *T*-Matrix formalism

The T-Matrix formalism has become nowadays a well-known technique to solve the multiple-scattering equations of an ensemble of spheres. It can also be used to evaluate the scattering properties of an arbitrary shaped particle constructed as a collection of spheres in contact. In this work, we use a previously developed RCTMA [5] to calculate the extinction cross section of clusters of different number of spheres, as well as with different overall shapes. In this section, we briefly recall the main features of the formalism.

3.1. Single scattering

The single T-matrix formalism and the associated extended-boundary-conditions technique were introduced by Watermann [6]. They allow the evaluation of the electromagnetic fields scattered by arbitrarily shaped particles, assuming elastic scattering. Applied to a sphere, the T-matrix formalism is equivalent to Mie theory. The incident $\mathbf{E}_{\text{inc}}$ and the scattered $\mathbf{E}_{\text{sca}}$ fields are both expanded on a spherical wave basis $Rg\mathbf{\Psi}_{\sigma nm}$ and $\mathbf{\Psi}_{\sigma nm}$ as follows:

$$\mathbf{E}_{\text{inc}} = \sum_{n}\sum_{m}\sum_{\sigma} a_{\sigma nm} Rg\mathbf{\Psi}_{\sigma nm}(k_0\mathbf{r}), \tag{4}$$

$$\mathbf{E}_{\text{sca}} = \sum_{n}\sum_{m}\sum_{\sigma} f_{\sigma mn}\mathbf{\Psi}_{\sigma nm}(k_0\mathbf{r}), \tag{5}$$

where $a_{\sigma nm}$ and $f_{\sigma mn}$ are the expansion coefficients, k_0 is the modulus of the wave vector in the medium and Rg means regular part (non-singular at the origin). One can show that one can express the scattering field coefficients $f_{\sigma mn}$ as functions of the incident field coefficients $a_{\sigma nm}$ through a simple relation: $\mathbf{f} = \mathbf{T}^{1(1)} \cdot \mathbf{a}$, where $\mathbf{T}^{1(1)}$ is the single T-matrix of the sphere, and $\mathbf{f}$ and $\mathbf{a}$ are column vectors with components $f_{\sigma mn}$ and $a_{\sigma nm}$, respectively.

3.2. Multiple scattering

In the multiple scattering formalism, the local (exciting) field $\mathbf{E}_{\text{loc}}^{i(N)}$ impinging on the ith particle is not only the incident radiation, it is the incident radiation plus the field scattered by all the other particles at the region occupied by ith particle. Each of the scattered fields is first expanded in a local spherical basis centered at each of the spheres, while the incident field is expanded in a spherical basis centered at a common origin. Since the scattered fields are expanded in a different basis to impose boundary conditions on the ith particle, one requires to translate them to a basis centered at the origin of the ith particle. These translations are performed using the translational matrices $\bar{\mathbf{J}}^{(i,0)}$ and $\bar{\mathbf{H}}^{(i,j)}$, introduced by Stein [7], where the superscripts $(i,0)$ and (i,j) mean translation from the common origin, and the center of the jth particle to the center of the ith particle, respectively. Therefore, one can expand the exciting field at the ith particle as

$$\mathbf{E}_{\text{loc}}^{i(N)} = Rg\mathbf{\Psi}^{\text{t}}(k_0|\mathbf{r}-\mathbf{r}_i|) \cdot \bar{\mathbf{J}}^{(i,0)} \cdot \mathbf{a} + \sum_{\substack{j=1 \\ j\neq i}}^{N} Rg\mathbf{\Psi}^{\text{t}}(k_0|\mathbf{r}-\mathbf{r}_i|) \cdot \bar{\mathbf{H}}^{(i,j)} \cdot \mathbf{f}^{j(N)}, \tag{6}$$

where the superscript t denotes transpose. As in the single T-matrix formalism, one can associate to each sphere a multiple T-matrix denoted by $\bar{\mathbf{T}}^{i(N)}$ that allows one to express the expansion coefficients of the scattered fields $\mathbf{f}^{i(N)}$ as a function of the incident-wave coefficients, through the relation $\mathbf{f}^{i(N)} = \bar{\mathbf{T}}^{i(N)} \cdot \mathbf{a}^{i}$. This multiple T-matrix takes into account all the multiple scattering interactions with all the other particles of the system. The knowledge of this T-matrix is the only requirement to calculate the total scattered field and to characterize the optical properties of the system. Using the definition of the single T-matrix and expression (6) for the local field, one can show that the multiple T-matrices are solutions of a linear system of N-coupled equations. This system can be solved by different techniques [8–11]. Here we use a RCTMA, recently developed by us, that combines

the recursive algorithm derived by Chew [12] and the centered T-matrix concept introduced by Mackowski [10]. The main idea is that the multiple T-matrix can be expressed in terms of centered T-matrices $\bar{\tau}_N^{(i,j)}$, through the following relation:

$$\bar{\mathbf{T}}^{i(N)} = \sum_{j=1}^{N} \bar{\tau}_N^{(i,j)} \cdot \bar{\mathbf{J}}^{(j,i)}, \quad i = 1, \ldots, N. \tag{7}$$

The evaluation of the centered T-matrices provide the ingredients for the calculation of the multiple-T matrices. The recursive algorithm to determine the $\bar{\tau}_N^{(i,j)}$ matrices is briefly described in Appendix A.

3.2.1. Optical coefficients

In this section we will regard, for simplicity, the crystallites as spheres and the aggregates as a cluster of touching spheres. We then calculate the extinction cross sections of this type of cluster. Let us recall that the extinction cross section is the sum of the scattering plus the absorption cross sections. Since in realistic circumstances, the cluster within the matrix will be randomly oriented, one actually requires the calculation of an orientation average of the extinction cross section, where the average is performed over all possible directions and polarization of the incident field. The first analytical relation for the average of the extinction cross section of a collection of spheres, using a T-matrix formalism, was introduced by Mackowski [13]. In our formalism, it has the following expression:

$$\langle C_{\text{ext}} \rangle = -\frac{2\pi}{k^2} Tr \left[\sum_{i=1}^{N} \sum_{j=1}^{N} \bar{\tau}_N^{(i,j)} \cdot \bar{\mathbf{J}}^{(j,i)} \right], \tag{8}$$

where $\langle \ldots \rangle$ denotes orientation average and the average is performed over the polarization states and over all the possible directions of the incident wave.

4. Results and discussion

Here we analyze the effects of clustering on the scattering efficiency by comparing the average extinction cross section of various clusters of particles with the total cross section of the same number of isolated particles. This analysis allows us to determine under which circumstances the aggregated system scatters more or less than the isolated particles. Also, in order to compare the scattering efficiency of clusters with different number of spheres, one calculates the average extinction cross section per unit volume (AECS/V), that is, one divides the extinction cross section by the total volume of the aggregate. We also study the validity of the equivalent-sphere approximation used in particle-sizing techniques like dynamic or static light scattering. We do this by calculating the AECS/V of a sphere with the same volume as the aggregate. Finally, we consider the influence of the shape of the aggregate on the scattering efficiency. Since the number of possible aggregate geometries is quite large, we focus our attention only on two extreme configurations: a 3D compact arrangement and a linear chain.

We now present results of the calculation of the AECS/V of different TiO_2 aggregates composed by 4, 8 and 13 identical spheres. The AECS/V's are plotted as a function of the size of the individual spheres forming the cluster. Since the spectral sensitivity of the human eye attains its maximum in

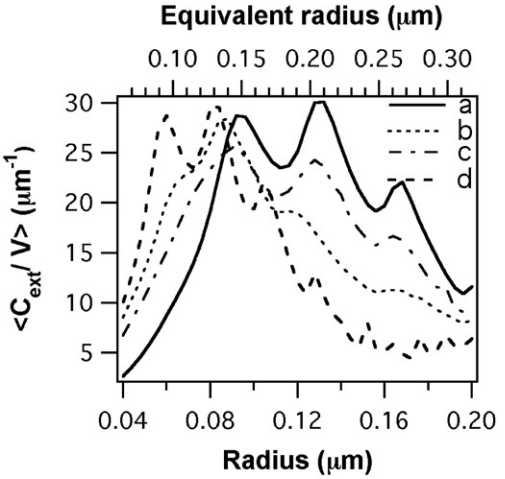

Fig. 2. AECS/V of a system of four spheres as a function of the size of each sphere: (a) isolated pigment; (b) compact configuration; (c) linear configuration; and (d) equivalent-sphere model.

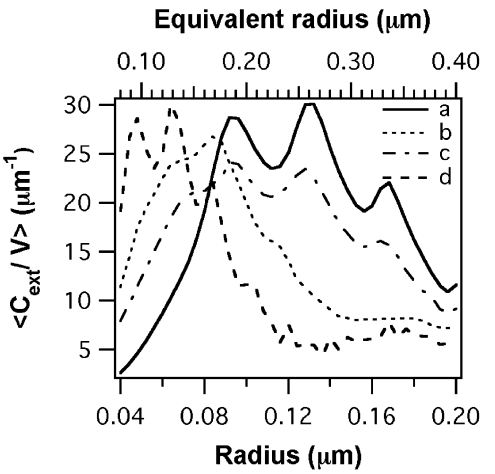

Fig. 3. AECS/V of a system of eight spheres as a function of the size of each sphere: (a) isolated pigment; (b) compact configuration; (c) linear configuration; and (d) equivalent-sphere model.

the green part of the spectrum, the wavelength of the incident radiation has been fixed at 0.546 μm in all calculations. The indices of refraction of the TiO_2 pigments and the surrounding medium are taken as 2.8 and 1.5, respectively. Since the indices of refraction are real, there is no absorption, and the extinction cross section coincides with the scattering cross section. Figs. 2–4 correspond to systems with clusters of 4, 8 and 13 spheres, where the different curves represent the (AECS/V) of (a) the isolated particles, (b) the compact and (c) linear configurations, and (d) the equivalent-sphere approximation. Notice that in this last case the scale of radii is located in the x-axis at the upper side of the frame.

Comparing the AECS/V's of isolated spheres with the ones of the aggregated systems one can identify two different, quite-well-separated regions. For a particle size of the constituents up to around 0.80–0.90 μm, which comprises the entire Rayleigh regime and the beginning of the first Mie resonance, the aggregated systems scatter more than the isolated particles. In this same region of particle sizes, where the size parameter is less than one, the compact structures scatter more than the linear ones.

Let us recall that the size parameter of the constituent spheres is defined as their radius over the wavelength of light in the surrounding medium, times 2π. For larger particle sizes, the aggregate systems start to scatter less efficiently than the isolated particles. This is at the beginning of the first Mie resonance of the isolated particles, where their size parameter is now larger than one. In this region of particle sizes there is also a change of behavior in relation to the shape of the aggregates, because in this region the compact configurations scatter now less than the linear ones. Also, in both regions of particle sizes, the difference in AECS/V between the compact and the linear configurations increases as the number of particles gets larger. One can also see that the linear aggregates keep the resonance structure linked to the excitation of the normal modes of the isolated particles, whereas in the compact ones they are washed out.

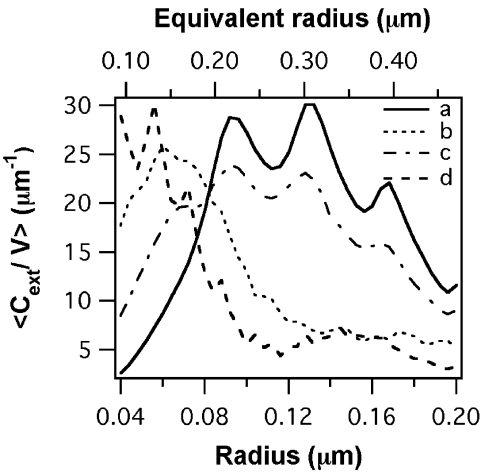

Fig. 4. AECS/V of a system of 13 spheres as a function of the size of each sphere: (a) isolated pigment; (b) compact configuration; (c) linear configuration; and (d) sphere equivalent volume.

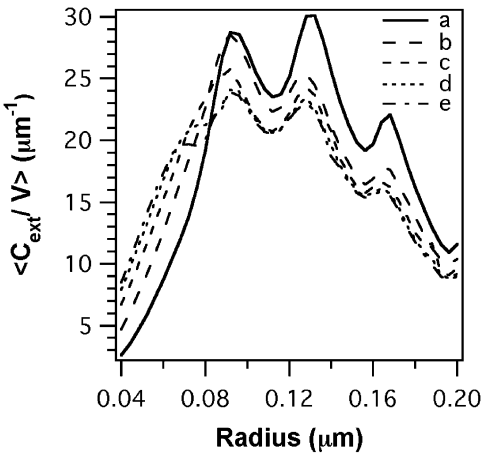

Fig. 5. AECS/V of the linear configurations as a function of the size of each sphere: (a) isolated pigment; (b) two spheres; (c) four spheres; (d) eight spheres; and (e) 13 spheres.

In relation to the comparison between the AECS/V's of the clusters and those corresponding to the equivalent-sphere model, our results show that this latter approximation has to be handle with care. The first expected observation is that the AECS/V's of the equivalent-sphere model are far from being a good approximation to the corresponding ones of the linear configurations, neither quantitatively, nor even qualitatively (except for very small sizes). On the contrary, in the whole range of sizes, there is qualitative agreement between the AECS/V's of the compact configurations and the corresponding ones of the equivalent-sphere model. However, the quantitative agreement is not very satisfactory except in a short range of large sizes. For very small sizes of the constituent spheres, the equivalent-sphere model overestimates the AECS/V's of the compact clusters while for large sizes the AECS/V's are underestimated. The boundary between these two regions lies around the location of the first Mie resonance of the isolated sphere.

In Figs. 5 and 6 we put together the AECS/V's of the linear and the compact configurations for 1, 2, 4, 8 and 13 spheres. One can observe a very different behavior of the AECS/V's between the compact and linear configuration, and the difference between them becomes larger as the number of spheres increases. In the compact case, and at large sizes of the constituent spheres, the AECS/V's decrease as the number of spheres gets larger, whereas the AECS/V's of the linear cluster approach a limit as the number of spheres in the cluster is increased. Obviously, this limit corresponds to the AECS/V of the infinite chain.

5. Conclusion

We have performed a study on the influence of the clustering process of rutile titanium dioxide particles in the hiding power of a paint. In a first approximation, clustering effects can be regarded

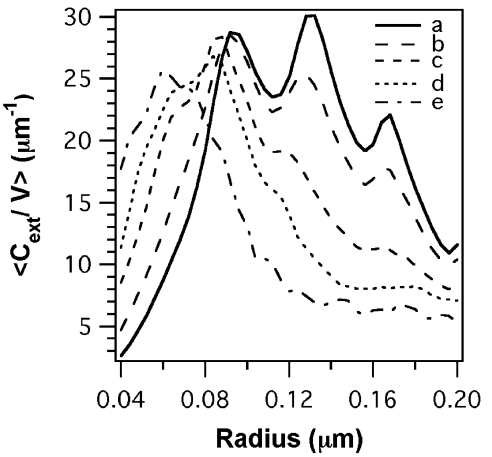

Fig. 6. AECS/V of the compact configurations as a function of the size of each sphere: (a) isolated pigment; (b) two spheres; (c) four spheres; (d) eight spheres; and (e) 13 spheres.

as a change in the particle-size distribution, where the clusters are regarded as spheres having the same volume as the clusters. This is what we called the equivalent-sphere model. Then we focused on the study of the average extinction cross section per unit volume (AECS/V) of various clusters as function of their size and geometry. We show how the clustering process could decrease tremendously the scattering efficiency of isolated particles by considering the case of two extreme aggregate geometries: a compact structure and a linear chain. Eventually, we show that the equivalent-sphere model should be handled with care, since this approximation for the scattering properties of compact clusters holds only qualitatively. Therefore, we conclude that a thorough study of the clustering phenomena in granular films should be done more extensively than the one presented here. One should consider a larger number of spheres in each cluster and, perhaps, different kinds of geometries taken, for example, from electron-microscope studies in real samples. Our study applied rutile titanium dioxide particles using parameters relevant to the paint industry, but it can be easily extended to other areas of research, as astrophysics, atmospheric physics or cosmetic systems by simply changing the indices of refraction of the particles and adjusting the size and geometries of the aggregates.

Acknowledgements

The authors wish to acknowledge the partial support given by Consejo Nacional de Ciencia y Tecnología through grant RI-1200-2-1 as well as the encouragement of Eduardo Nahmad.

Appendix A. RCTMA relations

First order of recurrence:

$$\bar{\tau}_N^{(1,1)} = [\bar{\mathbf{I}} - \bar{\mathbf{T}}^{1(1)} \cdot \bar{\mathbf{H}}^{(1,2)} \cdot \bar{\mathbf{T}}^{2(1)} \cdot \bar{\mathbf{H}}^{(2,1)}]^{-1} \cdot \bar{\mathbf{T}}^{1(1)},$$

$$\bar{\tau}_N^{(1,2)} = \bar{\tau}_N^{(1,1)} \cdot \bar{\mathbf{H}}^{(1,2)} \cdot \bar{\mathbf{T}}^{2(1)},$$

$$\bar{\tau}_N^{(2,2)} = [\bar{\mathbf{I}} - \bar{\mathbf{T}}^{2(1)} \cdot \bar{\mathbf{H}}^{(2,1)} \cdot \bar{\mathbf{T}}^{1(1)} \cdot \bar{\mathbf{H}}^{(1,2)}]^{-1} \cdot \bar{\mathbf{T}}^{2(1)},$$

$$\bar{\tau}_N^{(2,1)} = \bar{\tau}_N^{(2,2)} \cdot \bar{\mathbf{H}}^{(2,1)} \cdot \bar{\mathbf{T}}^{1(1)}.$$

Recurrence relation from $\bar{\mathbf{T}}^{N(N)}$ matrix:

$$\bar{\tau}_N^{(N,N)} = \left[\bar{\mathbf{I}} - \bar{\mathbf{T}}^{N(1)} \sum_{i=1}^{N-1} \bar{\mathbf{H}}^{(N,i)} \cdot \sum_{j=1}^{N-1} \bar{\tau}_{N-1}^{(i,j)} \cdot \bar{\mathbf{H}}^{(j,N)} \right]^{-1} \cdot \bar{\mathbf{T}}^{N(1)},$$

$$\bar{\tau}_N^{(N,j)} = \bar{\tau}_N^{(N,N)} \cdot \sum_{i=1}^{N-1} \bar{\mathbf{H}}^{(N,i)} \cdot \bar{\tau}_{N-1}^{(i,j)}, \quad j \neq N.$$

Recurrence relation from the $\bar{\mathbf{T}}^{k(N)}$ matrices, $k = 1, \ldots, N-1$:

$$\bar{\tau}_N^{(k,i)} = \bar{\tau}_{N-1}^{(k,i)} + \sum_{j=1}^{N-1} \bar{\tau}_{N-1}^{(k,j)} \cdot \bar{\mathbf{H}}^{(j,N)} \cdot \bar{\tau}_N^{(N,i)}, \ i \neq N,$$

$$\bar{\tau}_N^{(k,N)} = \sum_{j=1}^{N-1} \bar{\tau}_{N-1}^{(k,j)} \cdot \bar{\mathbf{H}}^{(j,N)} \cdot \bar{\tau}_N^{(N,N)}, \quad i = N.$$

$\bar{\mathbf{J}}^{(k,i)}$ and $\bar{\mathbf{H}}^{(k,i)}$ are the translational matrices which can be written as

$$\bar{\mathbf{J}}^{(k,i)} = \begin{bmatrix} RgA_{nm}^{\nu\mu(q)} & RgB_{nm}^{\nu\mu(q)} \\ RgB_{nm}^{\nu\mu(q)} & RgA_{nm}^{\nu\mu(q)} \end{bmatrix} \quad \text{and} \quad \bar{\mathbf{H}}^{(k,i)} = \begin{bmatrix} A_{nm}^{\nu\mu(q)} & B_{nm}^{\nu\mu(q)} \\ B_{nm}^{\nu\mu(q)} & A_{nm}^{\nu\mu(q)} \end{bmatrix}. \tag{A.1}$$

The $A_{nm}^{\nu\mu(q)}$ and $B_{nm}^{\nu\mu(q)}$ are the translation coefficients needed for the transformation from the ith to the kth coordinate system

References

[1] Bohren CF, Huffman DR. Absorption and scattering of light by small particles. New York: Wiley-Interscience Publication, 1983.

[2] Kubelka P, Munk F. Ein Beitrag zur Optik der Farbanstriche. Z Tech Phys (Leipzig) 1931;(12):593–601.

[3] Palik ED. Handbook of optical constants of solids. Boston, USA: Academic Press, 1985.

[4] Mishchenko MI, Hovenier JW, Travis LD. editors. Light scattering by nonspherical particles. New York: Academic Press, 2000.

[5] Auger JC, Stout B, Barrera RG. Scattering properties of rutile pigments located eccentrically within microvoids. JQSRT 2001;70:675–95.

[6] Waterman P. Symmetry unitary and geometry in electromagnetic scattering. Phys Rev D 1971;3(4):825–39.

[7] Stein S. Addition theorems for spherical wave functions. Q Appl Math 1961;19(1) : 15–24.

[8] Borghese F, Denti P, Saija R, Toscano G. Multiple electromagnetic scattering from a cluster of sphere I theory. Aerosol Sci Technol 1984;4:227–35.

[9] Hamid A. Electromagnetic scattering by an arbitrary configuration of dielectric spheres. Can J Phys 1990;68: 1419–28.
[10] Mackowski D, Mishchenko M. Calculation of the T-matrix and the scattering matrix for ensembles of spheres. J Opt Soc Am A 1996;13(11):2266–78.
[11] Xu Y. Electromagnetic scattering by an aggregate of sphere. Appl Opt 1995;34(21):4573–88.
[12] Chew W. Waves and fields in inhomogeneous media. IEEE Press Series on Electromagnetic Waves, 1990.
[13] Mackowski D. Calculation of total cross sections of multiple-sphere clusters. J Opt Soc Am A 1994;11(11): 2851–61.